Parton fragmentation into photons beyond the leading order

M. Glück, E. Reya, and A. Vogt
Institut für Physik, Universität Dortmund, D-4600 Dortmund 50, Federal Republic of Germany
(Received 1 February 1993)

Photon production via deep inelastic quark and gluon fragmentation is studied beyond the leading perturbative order within the framework of a specific factorization scheme (DIS_γ) chosen to provide the maximally possible amount of perturbative stability. It is argued that the perturbative (pointlike) results are expected to present a realistic estimate for photonic fragmentation functions, and the ambiguities related to the presently unknown, but possibly small, nonperturbative hadronic contributions are pointed out.

PACS number(s): 13.85.Qk, 12.38.Bx, 14.80.Am

I. INTRODUCTION

Direct photons produced in deep-inelastic (leptonic and hadronic) processes are often considered as a useful signal for investigating various aspects of the standard model. Usually the considered direct photon signal (e.g., of a hadronically produced intermediate-mass Higgs boson) must be separated from photonic backgrounds arising through the fragmentation of copiously produced quarks and gluons. The introduction of isolation cuts for the photon reduces the rate of these background events and simultaneously reduces the importance of the nonperturbative components involved in the partonic fragmentation into photons, provided the implemented isolation cuts are sufficiently high. A study of the nonisolated photonic fragmentation is, however, helpful in determining the size of the required isolation cuts. Moreover, recent measurements of isolated prompt photons at the Fermilab Tevatron [1] have shown that, despite the applied isolation cuts, these photonic fragmentation contributions may remain at least as important [2] as the "internal" photons produced directly in the hard subprocesses at small $x_T \equiv 2p_T^\gamma/\sqrt{s} \lesssim 10^{-2}$, i.e., for $p_T^\gamma \lesssim 20$ GeV. Beyond this more practical and urgent aspect, the study of photonic fragmentation processes is an interesting topic by itself within the framework of perturbative QCD, somewhat comparable to the closely related but more important photon structure functions.

The close relation, via crossing, between the timelike ($Q^2 \equiv q^2 > 0$) photonic fragmentation functions $D_f^\gamma(x,Q^2)$ and the spacelike ($Q^2 \equiv -q^2 > 0$) photon structure functions $f^\gamma(x,Q^2)$, where $f = q, \bar{q}, g$, enables us to adopt most of what has been learned for the spacelike situation to the corresponding timelike photon production processes. To utilize this (formal) similarity to its full extent we present in Sec. II a parallel treatment of both cases using a unified notation. In particular, we point out the common formal aspects as well as the concrete differences arising from the specific values of the correspondingly involved splitting functions and Wilson expansion coefficients. The one- and two-loop evolution equations of the photonic fragmentation functions in the n-moment space are discussed in Sec. III (with some of our main results for the timelike two-loop anomalous dimensions being given in the Appendix) and we compare their dominant singularity structure in the modified minimal subtraction scheme ($\overline{\text{MS}}$) with the one in a specific factorization scheme [deep-inelastic γ scattering (DIS_γ)] where troublesome $\overline{\text{MS}}$ poles (which destabilize the Q^2 evolutions) do not appear. The quantitative implications for the photon production processes are discussed in Sec. IV; in particular, the perturbative stability of the predicted photonic fragmentation functions and the ambiguities due to the presently unknown, but possibly small hadronic contributions are pointed out. Our conclusions are summarized in Sec. V.

II. SPACE- AND TIMELIKE PHOTONIC STRUCTURE FUNCTIONS

The analysis of photonic structure functions, in particular, at higher orders of perturbative QCD, is intimately related to the appropriate definition of the so-called hadronic part, which is uniquely specified by stating the postulated boundary conditions [3,4] for the (input) distributions *as well as* the specific factorization scheme in which these boundary conditions are implemented [5,6]. The latter is traditionally [3,4] fixed in the $\overline{\text{MS}}$ factorization scheme with

$$f_r^{(S,T)}(x,Q^2) = \sum_q e_q^2 \left[q^{(S,T)}(x,Q^2) + \bar{q}^{(S,T)}(x,Q^2) + \frac{\alpha_s(Q^2)}{2\pi} [C_{q,r}^{(S,T)} * (q^{(S,T)} + \bar{q}^{(S,T)}) + 2C_{g,r}^{(S,T)} * g^{(S,T)}] + 2e_q^2 \frac{\alpha}{2\pi} C_{\gamma,r}^{(S,T)}(x) \right] + f_{r,h}^{(S,T)}(x,Q^2) , \tag{2.1}$$

 ©1993 The American Physical Society

where $f_1^{(S)}=2F_1^\gamma$, $f_2^{(S)}=F_2^\gamma/x$ for the spacelike (S) deep-inelastic process $\gamma^*(Q^2)\gamma\to X$, and $f_r^{(T)}$ are the corresponding structure functions for the timelike (T) reaction $\gamma^*(Q^2)\to\gamma X$. The summation extends over all light quarks, lying well below the kinematical threshold of heavy quark production, whose number is denoted, as usual, by f. The contribution of the heavy flavors near threshold is entailed in $f_{r,h}^{(S,T)}$ and specified, e.g., in Ref. [5] for the spacelike situation of the photon structure function. The convolutions in (2.1) are defined as usual:

$$C*q=\int_x^1\frac{dy}{y}C\left[\frac{x}{y}\right]q(y,Q^2) \tag{2.2}$$

and

$$\frac{\alpha_s(Q^2)}{4\pi}\simeq\frac{1}{\beta_0\ln(Q^2/\Lambda^2)}-\frac{\beta_1}{\beta_0^3}\frac{\ln\ln(Q^2/\Lambda^2)}{[\ln(Q^2/\Lambda^2)]^2}\ , \tag{2.3}$$

with $\beta_0=11-2f/3$ and $\beta_1=102-38f/3$. The notation chosen in (2.1) illuminates the close relationship between the timelike photonic fragmentation functions ($q^{(T)}\equiv D_q^\gamma$, $g^{(T)}\equiv D_g^\gamma$) and the well-known spacelike photonic parton distributions ($q^{(S)}\equiv q^\gamma$, $g^{(S)}\equiv g^\gamma$) which will be kept throughout, unless stated otherwise. The coefficient functions in the $\overline{\text{MS}}$ factorization scheme are [7–9]

$$\begin{aligned}
C_{q,2}^{(S)}&=C_F\left[\frac{1+x^2}{1-x}\left[\ln\frac{1-x}{x}-\frac{3}{4}\right]+\frac{1}{4}(9+5x)\right]_+\ ,\\
C_{q,1}^{(S)}&=C_{q,2}^{(S)}-C_F(2x)\ ,\\
C_{q,2}^{(T)}&=C_{q,2}^{(S)}+C_F\left[\frac{3(1+x^2)}{1-x}\ln x-\frac{7}{2}(1+x)\right.\\
&\qquad\left.+\pi^2\delta(1-x)\right]\ ,\\
C_{q,1}^{(T)}&=C_{q,2}^{(T)}+C_F(2)\ ,
\end{aligned} \tag{2.4}$$

and

$$\begin{aligned}
C_{g,2}^{(S)}&=T_R\left[[x^2+(1-x)^2]\ln\frac{1-x}{x}-1+8x(1-x)\right]\ ,\\
C_{g,1}^{(S)}&=C_{g,2}^{(S)}-T_R[4x(1-x)]\ ,\\
C_{g,2}^{(T)}&=C_F\left[\frac{1+(1-x)^2}{x}[\ln(1-x)+2\ln x]-6\frac{1-x}{x}\right]\ ,\\
C_{g,1}^{(T)}&=C_{g,2}^{(T)}+C_F\left[4\frac{1-x}{x}\right]\ ,
\end{aligned} \tag{2.5}$$

with $C_F=\frac{4}{3}$ and $T_R=\frac{1}{2}$. The photonic Wilson coefficients $C_{\gamma,r}^{(S,T)}$ in (2.1) are obtained from the gluonic ones by an obvious replacement of the color factors C_F and T_R:

$$C_{\gamma,r}^{(S)}=(3/T_R)C_{g,r}^{(S)}\ ,\quad C_{\gamma,r}^{(T)}=(1/C_F)C_{g,r}^{(T)}\ . \tag{2.6}$$

It should be noted that the higher-order universal (logarithmic) contributions to $C_{\gamma,r}^{(S,T)}$ in (2.1) develop negative spikes as $x\to1$, and a stronger one as $x\to0$ for the timelike case, which destabilize the perturbative expansion of the predictions for $f_r^{(S,T)}$ as obtained for similar leading-order (LO) and higher-order (HO) hadronic inputs for the distributions at some $Q^2=Q_0^2$ in the $\overline{\text{MS}}$ factorization scheme. As noted recently [5,6], perturbative stability is regained by considering a different factorization scheme, DIS_γ, in which the troublesome $C_{\gamma,2}^{(S)}$ term in the photon structure function $f_2^{(S)}$ in (2.1) is removed by absorbing it into the definition of the photonic (anti)quark distributions. In this new scheme the photonic distributions are, in general, defined by

$$q^{(S,T)}(x,Q^2)|_{\text{DIS}_\gamma}=q^{(S,T)}(x,Q^2)+e_q^2\frac{\alpha}{2\pi}C_{\gamma,r'}^{(S,T)}(x)\ , \tag{2.7}$$

with an identical expression for the antiquarks, whereas the gluon distributions remain unchanged, i.e., are the same as in $\overline{\text{MS}}$. An inspection of (2.1) shows that

$$C_{\gamma,r}^{(S,T)}|_{\text{DIS}_\gamma}=C_{\gamma,r}^{(S,T)}-C_{\gamma,r'}^{(S,T)}\ , \tag{2.8}$$

for which the aforementioned $x\to1$ and $x\to0$ instabilities are eliminated. In our former [5,6] calculations for the spacelike situation we have chosen $r'=2$ not only because $f_2^{(S)}=F_2^\gamma/x$ refers directly to the experimentally measured photon structure function, but also in order to maintain some analogy to the hadronic parton distributions where this convention is motivated [7] by the Adler sum rule. For our subsequent timelike calculations we choose $r'=1$ in (2.7) and (2.8) motivated by momentum sum rule considerations for fragmentation functions [8] which are directly related to $f_1^{(T)}$. In other words, we adopt the factorization scheme prescriptions of Ref. [7,8] for $C_{g,r'}^{(S,T)}$, as inspired by these sum rules, to the analogous [cf. Eq. (2.6)] photonic quantities $C_{\gamma,r'}^{(S,T)}$. It turns out that choosing $f_1^{(T)}$ for defining the DIS_γ scheme in (2.8) in the timelike region also provides the (almost) greatest possible perturbative stability. Having eliminated the troublesome perturbative instabilities, one can now implement *similar LO and HO inputs* at $Q^2=Q_0^2$ provided these inputs are imposed for the distributions as *defined in terms of the DIS_γ factorization scheme.*

As was further noted in Ref. [5], the Q^2 evolution of the DIS_γ distributions differs from that of the $\overline{\text{MS}}$ distributions $q^{(S,T)}$ and $g^{(S,T)}$ due to a corresponding transformation of the inhomogeneous k terms appearing in the evolution equations

$$\frac{dq^{(S,T)}(x,Q^2)}{d\ln Q^2}=k^{(S,T)}(x,Q^2)+P^{(S,T)}*q^{(S,T)}\ , \tag{2.9}$$

where the photon-parton splitting functions $k(x,Q^2)$ and the purely hadronic splitting functions $P(x,Q^2)$ receive the following one- and two-loop contributions:

$$\begin{aligned}
k(x,Q^2)&=\frac{\alpha}{2\pi}k^{(0)}(x)+\frac{\alpha\alpha_s(Q^2)}{(2\pi)^2}k^{(1)}(x)\ ,\\
P(x,Q^2)&=\frac{\alpha_s(Q^2)}{2\pi}P^{(0)}(x)+\left[\frac{\alpha_s(Q^2)}{2\pi}\right]^2P^{(1)}(x)\ .
\end{aligned} \tag{2.10}$$

Here $q^{(S,T)}$ denotes, as usual, either the flavor nonsinglet

(NS) combination

$$q_{\rm NS}^{(S,T)}=(q^{(S,T)}+\bar{q}^{(S,T)})-(1/f)\Sigma^{(S,T)}\ , \tag{2.11}$$

with $\Sigma^{(S,T)}\equiv\sum_f(q^{(S,T)}+\bar{q}^{(S,T)})$, or the flavor-singlet vector

$$\mathbf{q}^{(S,T)}=\begin{pmatrix}\Sigma^{(S,T)}\\ g^{(S,T)}\end{pmatrix}\ . \tag{2.12}$$

The corresponding splitting functions are $k_{\rm NS}^{(S,T)}$, $P_{\rm NS}^{(S,T)}$ and

$$\mathbf{k}^{(S,T)}=\begin{pmatrix}k_q^{(S,T)}\\ k_g^{(S,T)}\end{pmatrix}\ ,\quad \hat{P}^{(S)}=\begin{pmatrix}P_{qq}^{(S)} & P_{qg}^{(S)}\\ P_{gq}^{(S)} & P_{gg}^{(S)}\end{pmatrix}\ , \tag{2.13}$$

$$\hat{P}^{(T)}=\begin{pmatrix}P_{qq}^{(T)} & P_{gq}^{(T)}\\ P_{qg}^{(T)} & P_{gg}^{(T)}\end{pmatrix}\ .$$

All these splitting functions are well known in Bjorken-x space up to the two-loop order [5,10–14] and are, for convenience, collected and appropriately presented in Sec. A 1.

Substituting now the transformation (2.7) into the evolution equations (2.9) one notes that the inhomogeneous k terms transform according to [5]

$$\begin{aligned}
k_q^{(1)(S,T)}(x)|_{\rm DIS_\gamma}&=k_q^{(1)(S,T)}(x)-e_q^2P_{qq}^{(0)}*C_{\gamma,r}^{(S,T)}\ ,\\
k_g^{(1,S)}(x)|_{\rm DIS_\gamma}&=k_g^{(1,S)}(x)-2f\langle e^2\rangle P_{gq}^{(0,S)}*C_{\gamma,2}^{(S)}\ ,\\
k_g^{(1,T)}(x)|_{\rm DIS_\gamma}&=k_g^{(1,T)}(x)-2f\langle e^2\rangle P_{qg}^{(0,T)}*C_{\gamma,1}^{(T)}\ ,
\end{aligned} \tag{2.14}$$

with $\langle e^2\rangle\equiv f^{-1}\sum_f e_q^2$ and

$$\begin{aligned}
P_{qq}^{(0)}(x)&=C_F\left[\frac{1+x^2}{1-x}\right]_+\ ,\\
P_{gq}^{(0,S)}(x)&=C_F\frac{1+(1-x)^2}{x}\ ,\\
P_{qg}^{(0,T)}(x)&=T_R[x^2+(1-x)^2]\ .
\end{aligned} \tag{2.15}$$

These transformations have the additional merit of canceling the dominant $1/x$ and $\ln x/x$ singularities of $k_g^{(1,S)}$ and $k_g^{(1,T)}$ in Eq. (A3), respectively, which destabilize the perturbative expansion of the Q^2 evolution for the photonic distributions in the medium- to small-x region. The explicit verification of the singularity cancellations is easily achieved and most transparent in the Mellin n-moment space to which we now turn.

III. THE EVOLUTION EQUATIONS FOR MOMENTS OF PARTON DENSITIES AND THEIR DOMINANT SINGULARITY STRUCTURE

In the n-moment space, defined by the Mellin transformation

$$f(n)\equiv\int_0^1 dx\,x^{n-1}f(x)\ , \tag{3.1}$$

the integral convolutions in (2.9) and (2.14) reduce to simple products of the corresponding n moments. This allows for explicit analytic solutions [5] of the evolution equations, in contrast to their Bjorken-x version (2.9), which moreover allow for simply retaining only those α_s terms relevant for a consistent next-to-leading order analysis [5]. These moment expressions can then be easily (numerically) Mellin inverted to x space [5]. Apart from being theoretically more transparent, this method of solving the evolution equations is very efficient and stable in the low-x and/or high-Q^2 region since it avoids the many numerical iterations involved in the more direct but purely numerical Bjorken-x space calculation. (This situation is similar to the one encountered for nucleon structure functions [15,16].) The n moments of all required one- and two-loop splitting functions in the spacelike region (i.e., for calculating photonic parton distributions) are well known and conveniently presented in [5]. Since this is not the case for the timelike situation (photonic fragmentation functions), we have calculated the moments of all photonic and hadronic two-loop splitting functions and Wilson coefficients which are presented in Sec. A 2.

The dominant (as $x\to 0$) $1/x$ and $\ln x/x$ singularities of $k_g^{(1,S)}$ and $k_g^{(1,T)}$ in (A3), respectively, mentioned at the end of the previous section, correspond to the $1/(n-1)$ and $-1/(n-1)^2$ poles of $k_g^{(1,S)}(n)$ and $k_g^{(1,T)}(n)$ presented in the Appendix. Some of these troublesome poles of $k_{g,q}^{(1)}$ in the $\overline{\rm MS}$ scheme, which mostly destabilize the perturbative expansion for the solution of the Q^2-evolution equations, do however *vanish for* $k_{g,q}^{(1)}|_{DIS_\gamma}$ in (2.14). This property is of particular importance for $k_g^{(1,T)}$ whose negative $\overline{\rm MS}$ $\ln x/x$ contribution in (A3) for small x seriously affects [11] $D_g^\gamma(x,Q^2)$, thereby acquiring physically unacceptable negative values in the medium- to small-x range. This disturbing feature of D_g^γ, arising in the $\overline{\rm MS}$ factorization scheme, disappears in the $\rm DIS_\gamma$ scheme as can be demonstrated analytically by identifying the dominant $x\to 0$ singularities of $k^{(1)}(x)$ or equivalently and more conveniently the rightmost poles of the moments $k^{(1)}(n)$.

For completeness let us start with the dominant poles for the spacelike case relevant for the photon structure functions [5]. According to Eq. (2.14), using the relevant moment expressions of Sec. A 2, the *dominant* $n=1$ pole term in $k_g^{(1,S)}$ *cancels* due to $C_{\gamma,2}^{(S)}(n=1)=1$ and, furthermore, the subdominant $1/n^3$ pole is canceled as well:

$$\begin{aligned}
k_g^{(1,S)}(n)|_{\rm DIS_\gamma}&=k_g^{(1,S)}(n)-2f\langle e^2\rangle P_{gq}^{(0,S)}(n)C_{\gamma,2}^{(S)}(n)\\
&=f\langle e^2\rangle C_F\left[3\frac{4}{3}\frac{1}{n-1}-2\frac{2}{n-1}C_{\gamma,2}^{(S)}-O(1/n^3)\right]\\
&=f\langle e^2\rangle C_F[(12/n^2)+O(1/n)]\ ,
\end{aligned} \tag{3.2}$$

to be compared with the more singular $\overline{\text{MS}}$ quantity

$$k_g^{(1,S)}(n)=4f\langle e^2\rangle C_F/(n-1)-O(1/n^3)$$

corresponding to

$$k_g^{(1,S)}(x)\simeq 3f\langle e^2\rangle C_F(4/3x)$$

as $x\to 0$ in (A3). It is interesting to note that the leading $x\to 0$ singularity of the singlet

$$k_q^{(1,S)}(x)\simeq 3f\langle e^2\rangle C_F[\ln^2 x+O(\ln x)]$$

in (A3), or equivalently

$$k_q^{(1,S)}(n)\simeq 3f\langle e^2\rangle C_F[2/n^3-O(1/n^2)]\ ,$$

gets also canceled in the DIS_γ scheme as can be easily verified from Eq. (2.14):

$$k_q^{(1,S)}(n)|_{\text{DIS}_\gamma}=f\langle e^2\rangle C_F[-(6/n^2)+O(1/n)]\ . \tag{3.3}$$

Thus the DIS_γ scheme does not only remove the $x\to 1$ instabilities in $f_r^{(S,T)}$, but also simultaneously tames the $x\to 0$ singularities of the distributions. This is mainly responsible for stabilizing the HO results [5] with respect to the LO ones, in contrast with the $\overline{\text{MS}}$ scheme. It should be noted that the dominant singularity would not have canceled in (3.2) if we had used $C_{\gamma,1}^{(S)}$, i.e., $r'=1$ in (2.7) for the spacelike case, which is theoretically disfavored as discussed after Eq. (2.8).

The small-x singularities in the timelike region are far more serious [11] in the $\overline{\text{MS}}$ scheme: As $x\to 0$,

$$k_g^{(1,T)}(x)\simeq f\langle e^2\rangle T_R[(16/3x)\ln x+O(1/x)]$$

according to Eq. (A3), which corresponds to the singular $-\frac{16}{3}(n-1)^{-2}$ term of $k_g^{(1,T)}(n)$ in Eq. (A13). This *dominant* $n=1$ singularity is again *canceled* in the DIS_γ scheme where, due to Eq. (2.14),

$$\begin{aligned}k_g^{(1,T)}(n)|_{\text{DIS}_\gamma}&=k_g^{(1,T)}(n)-2f\langle e^2\rangle P_{qg}^{(0,T)}(n)C_{\gamma,1}^{(T)}(n)\\&=f\langle e^2\rangle\left[T_R\left[-\frac{16}{3}\frac{1}{(n-1)^2}+\frac{92}{9}\frac{1}{n-1}\right]-2P_{qg}^{(0,T)}(n)\left[-\frac{4}{(n-1)^2}-\frac{2}{n-1}\right]+O\left[\frac{1}{n^3}\right]\right]\\&=f\langle e^2\rangle T_R\left[\frac{64}{9}\frac{1}{n-1}+O\left[\frac{1}{n^3}\right]\right]\ ,\end{aligned} \tag{3.4}$$

where we have used the appropriate moment expressions presented in Sec. A 2 and the Taylor expansion around $n=1$,

$$P_{qg}^{(0,T)}(n)\simeq T_R[2/3-13(n-1)/18]\ .$$

From (3.4) we see that the $(n-1)^{-2}$ singularity gets entirely canceled in DIS_γ and that the size of the next-to-leading $(n-1)^{-1}$ pole is reduced to $\frac{64}{9}(n-1)^{-1}$, as compared to the subleading $\frac{92}{9}(n-1)^{-1}$ term in the $\overline{\text{MS}}$ scheme in (A13), which corresponds to $64/9x$ in $k_g^{(1,T)}(x)|_{\text{DIS}_\gamma}$. Thus, the huge instability encountered in Ref. [11] for the perturbative predictions for $D_g^\gamma(x,Q^2)$, where D_g^γ becomes even negative mainly because of the dominant $(16/3x)\ln x$ term in $k_g^{(1,T)}$, disappears in the DIS_γ scheme as will be demonstrated quantitatively in the next section. On the other hand, the small-x behavior of

$$k_q^{(1,T)}(x)\simeq 2f\langle e^2\rangle C_F\ln^2 x$$

in Eq. (A3), which corresponds to the $+2/n^3$ term in (A12), becomes worse in the DIS_γ scheme where Eq. (2.14) gives, using

$$P_{qq}^{(0)}(n)\simeq C_F(5/4-\pi^2/3)(n-1)$$

around $n=1$,

$$k_q^{(1,T)}(n)|_{\text{DIS}_\gamma}\simeq 2f\langle e^2\rangle C_F\left[\left[5-\frac{4\pi^2}{3}\right]\frac{1}{n-1}-\frac{2}{n^3}\right]\ , \tag{3.5}$$

which corresponds to the more singular small-x behavior $(5-4\pi^2/3)/x-2\ln^2 x$. (A $1/x$ singularity is already present in the LO $k_q^{(0,T)}$). This, however, does not destabilize the perturbative HO results in the DIS_γ scheme too seriously since $k_q^{(1)}$ is subleading as compared to $k_q^{(0)}$ in Eq. (A2), in contrast with $k_g^{(1)}$ which dominates due to $k_g^{(0)}=0$. It should be noted that the dominant pole in (3.4) would also be canceled if the theoretically disfavored $C_{\gamma,2}^{(T)}$ were used, as discussed after Eq. (2.8), but the strength of the remaining $(n-1)^{-1}$ pole would have increased from $\frac{64}{9}$ to $\frac{112}{9}$ in Eq. (3.4).

The aforementioned singularity cancellations are due to the fact that they belong to just those two-loop graph contributions to $k^{(S,T)}$ corresponding to the convolution terms in (2.14) whose subtraction actually corrects the unphysical features entailed in the $\overline{\text{MS}}$ factorization scheme which artificially separates two components of $f_{r,h}$ in the limit $m_h\to 0$. One should, in fact, recall that the above-mentioned separation into a HO C_γ term and a leading order $k^{(0)}$ term induces a different Q^2 behavior of two pieces which were originally combined in the single, regular, and positive $f_{r,h}$. The DIS_γ factorization scheme restores the unity of the two pieces by bringing them together as components of k in (2.10) with C_γ absorbed into $k^{(1)}|_{\text{DIS}_\gamma}$. It is just this reunification which lies at the root of the *double* success of the DIS_γ factorization scheme, namely, the stabilization of the perturbative expansion of $F_r^\gamma(x,Q^2)$ as well as the simultaneous stabilization of the perturbative expansion for the distributions Σ^γ and g^γ as

shown in Figs. 1–3 of Ref. [5] for the spacelike situation where $r'=2$ in (2.7) yielded optimal perturbative stability. As was furthermore shown, for spacelike configurations [17], the stabilization of the perturbative expansion for the various cross sections is universal and not restricted to F_r^γ alone. One could, of course, expect this to also hold true for timelike situations involving photonic fragmentation functions since, as noted above, the troublesome $n=1$ negative dipole singularity in $k_g^{(1,T)}$ vanishes in the $\overline{\text{DIS}}_\gamma$ factorization scheme.

IV. NUMERICAL RESULTS

The predictions for $D_f^\gamma(x,Q^2)$ afford a specification of $D_f^\gamma(x,Q_0^2)$, where $f=q,\bar{q},g$. A measure for the perturbative stability of various factorization schemes is provided by choosing the same $D_f^\gamma(x,Q_0^2)$ for the LO and HO analysis, e.g.,

$$D_f^\gamma(x,Q_0^2\simeq 1\ \text{GeV}^2)=0\ , \tag{4.1}$$

usually referred to as the pointlike component or solution [3,4]. The boundary conditions (4.1) at $Q_0^2=1$ GeV^2, which determine $D_f^\gamma(x,Q^2>Q_0^2)$, correspond to situations in which the emitted photon is isolated [11,18,19] from its parent parton f by a p_T cut. The scale Q_0 should then be identified with the minimal relative transverse momentum, i.e., $Q_0=(p_T^{\gamma f})_{\min}$. For $(p_T^{\gamma f})_{\min}\gtrsim 1$ GeV one expects that all nonperturbatively generated photons are exponentially suppressed [1] as expressed by (4.1). As noted in the previous section, the $\overline{\text{DIS}}_\gamma$ factorization scheme needed for stabilizing the perturbative predictions of $f_1^{(T)}(x,Q^2)$ and of $D_g^\gamma(x,Q^2)$ in the whole x region, induces a slight destabilization of $D_q^\gamma(x,Q^2>Q_0^2)$ with respect to the $\overline{\text{MS}}$ scheme. To illustrate these points we present in Figs. 1–3 the perturbative predictions, using (4.1), for $f=3$ active flavors with $\Lambda_{\text{LO}}^{(3)}=232$ MeV and $\Lambda_{\text{HO}}^{(3)}=248$ MeV corresponding to $\Lambda_{\text{LO}}^{(4)}=\Lambda_{\text{HO}}^{(4)}=200$ MeV. We show the resulting $f_1^{(T)}(x,Q^2)$ of Eq. (2.1),

$$D_\Sigma^\gamma(x,Q^2)\equiv\sum_f(D_q^\gamma+D_{\bar{q}}^\gamma)\ , \tag{4.2}$$

and $D_g^\gamma(x,Q^2)$ at $Q^2=5$ and 100 GeV^2 as calculated in leading (LO) and higher (HO) order, with the latter calculated, using (4.1), in the $\overline{\text{MS}}$ factorization scheme (in this context, formerly [5] named $\overline{\text{MS}}_{\text{naive}}$) as well as in the $\overline{\text{DIS}}_\gamma$ scheme with $r'=1$ in Eq. (2.7). As expected, the perturbative stability properties of the $\overline{\text{DIS}}_\gamma$ factorization scheme are superior to those of the $\overline{\text{MS}}$ scheme despite the somewhat unsatisfactory situation in the quark sector shown in Fig. 2. In the gluon sector, however, the (physically) disastrous negative $\overline{\text{MS}}$ results in Fig. 3 for $D_g^\gamma(x,Q^2)$, discovered originally in Ref. [11], disappear in the $\overline{\text{DIS}}_\gamma$ scheme. This unphysical negative $\overline{\text{MS}}$ result is caused mainly by the inhomogeneous $k_g^{(1,T)}$ term, which is negative throughout the whole x region (which is far worse than stated in Ref. [11]) and becomes singular as $\ln x/x$ for $x\to 0$. Similarly, the perturbative stability of the pointlike HO $\overline{\text{DIS}}_\gamma$ results for $f_1^{(T)}$, shown in Fig. 1, with respect to the LO ones, is particularly satisfactory in contrast with the $\overline{\text{MS}}$ predictions. It should be noted that

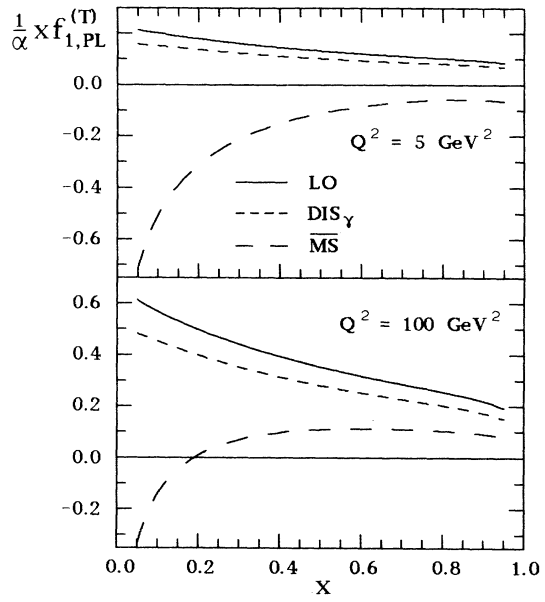

FIG. 1. The pointlike LO and HO solutions (for just $f=3$ active flavors) for the timelike photonic e^+e^- structure function $f_1^{(T)}$ defined in (2.1) in the $\overline{\text{DIS}}_\gamma$ and the (more singular) $\overline{\text{MS}}$ scheme. These results are obtained for the vanishing input (4.1) at $Q_0^2=1$ GeV^2 implemented correspondingly for the $\overline{\text{DIS}}_\gamma$ and the $\overline{\text{MS}}$ distributions.

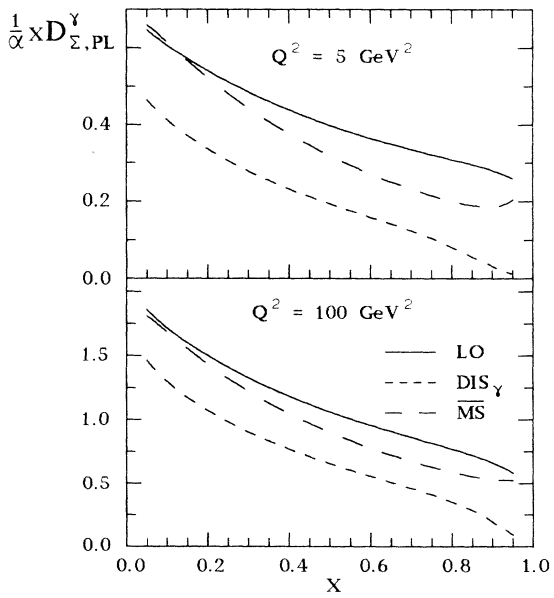

FIG. 2. The pointlike LO and HO ($f=3$) photonic flavor-singlet quark fragmentation functions, which also enter the predictions in Fig. 1, corresponding to the input (4.1) implemented for the $\overline{\text{DIS}}_\gamma$ and $\overline{\text{MS}}$ distributions at $Q_0^2=1$ GeV^2, relevant for isolated photon production. Note that the more common notation is $x\equiv z$.

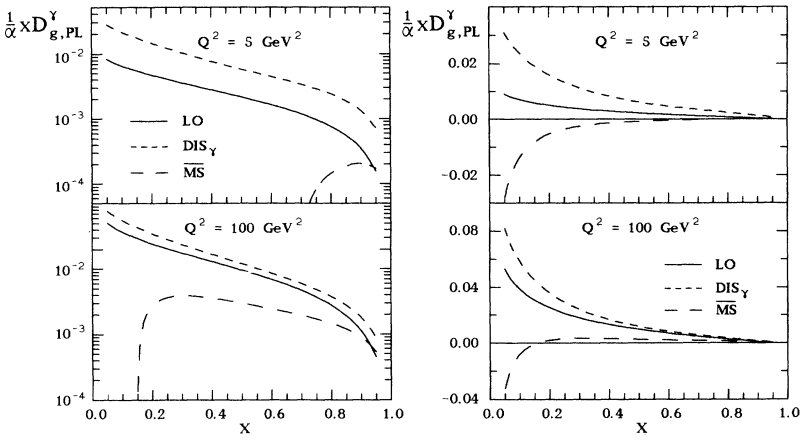

FIG. 3. As in Fig. 2 but for the pointlike photonic gluon fragmentation function, corresponding to the input (4.1), plotted on a (a) logarithmic and (b) linear scale.

the perturbative stability of the directly measurable $f_i^{(T)}$ in e^+e^- experiments is superior to the one of the theoretical quantities D_f^γ which also depend, in HO, on the definition chosen for the hadronic Wilson coefficients in Eq. (2.1) and that, furthermore, the negativity of the *physical* quantity $f_1^{(T)}$ in the $\overline{\text{MS}}$ scheme is unacceptable. Strictly speaking we have considered here only the perturbative pointlike hadronic part of $f_1^{(T)}$, corresponding to (4.1), which should be supplemented by the nonperturbative hadronic component. As noted in Refs. [5,6] for the case of photon structure functions and photonic quark and gluon distributions, as well as in Secs. II and III above, the favorable results for the pointlike component in the DIS$_\gamma$ factorization scheme allow for a reasonable specification of the nonperturbative hadronic component, e.g., in Eq. (4.6) below, also for the HO analysis (with the HO hadronic input being comparable but not drastically different from the LO one) in contrast with the situation in the $\overline{\text{MS}}$ factorization scheme (cf. Ref. [5]).

Because of these superior perturbative stability properties, we shall adopt the DIS$_\gamma$ scheme for our subsequent calculations based on (4.1) or some similar boundary conditions. For actual HO analyses of direct photon production in purely hadronic (or lepton-proton) reactions, however, one uses the $\overline{\text{MS}}$ scheme [11,18] where the various HO subprocesses have been calculated. In this case one should, of course, also transform the photonic DIS$_\gamma$ distributions, satisfying (4.1), into the $\overline{\text{MS}}$ scheme according to Eq. (2.7) [20]:

$$D^\gamma_{q,\bar{q}}(x,Q^2)|_{\overline{\text{MS}}}=D^\gamma_{q,\bar{q}}(x,Q^2)|_{\text{DIS}_\gamma}-e_q^2\frac{\alpha}{2\pi}C^{(T)}_{\gamma,1}(x)\ , \tag{4.3}$$

$$D^\gamma_g(x,Q^2)|_{\overline{\text{MS}}}=D^\gamma_g(x,Q^2)|_{\text{DIS}_\gamma}\ .$$

For illustration we show our pointlike DIS$_\gamma$ results as transformed to the $\overline{\text{MS}}$ scheme in Fig. 4. It is interesting to note that our predictions for D_u^γ in Fig. 4 are, as can be inferred from Fig. 2, about twice as large as the ones obtained by working throughout within the framework of the $\overline{\text{MS}}$ factorization scheme [11] with the more singular evolution equations as discussed in Sec. II. Since in Fig. 4 we show our predictions also at $Q^2=10^4$ GeV^2, the heavy flavors have been included, following our previous procedure [6] utilizing $m_{c,b}=1.5$ and 4.5 GeV for the heavy quark thresholds and

$$\Lambda^{(3,4,5)}_{\text{LO}}=232,\ 200,\ \text{and}\ 153\ \text{MeV}\ ,$$
$$\Lambda^{(3,4,5)}_{\text{HO}}=248,\ 200,\ \text{and}\ 131\ \text{MeV} \tag{4.4}$$

for the scales in $\alpha_s(Q^2)$ for the corresponding $f=3,4,5$ flavor regions.

For inclusive direct photon production (i.e., with no isolation cuts) the scale Q_0 from which the photonic radiation should be started is rather low [11], just as in the corresponding situation for the photon structure function

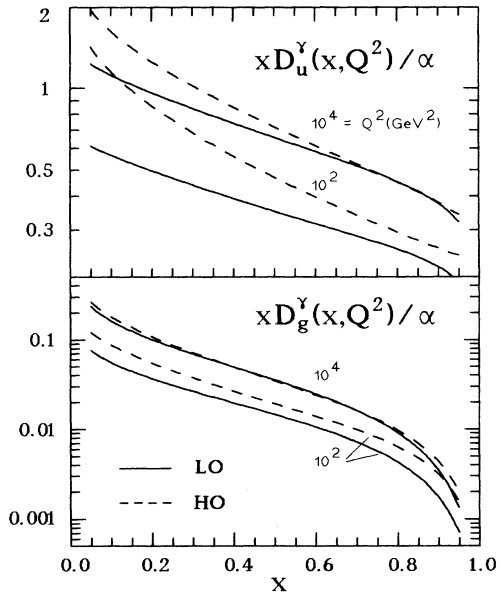

FIG. 4. Photonic LO and HO DIS$_\gamma$ fragmentation functions corresponding to the vanishing input at $Q_0^2=1$ GeV^2 in (4.1), relevant for isolated photon production; the contributions from the onset of heavy quark thresholds have been included as discussed in the text. All DIS$_\gamma$ results have been transformed into the $\overline{\text{MS}}$ scheme according to (4.3).

[6,21] where [6] $Q_0^2=\mu^2$ with

$$\mu_{\rm LO}^2=0.25\ {\rm GeV}^2\ ,\quad \mu_{\rm HO}^2=0.3\ {\rm GeV}^2\ , \tag{4.5}$$

henceforth also adopted for the LO and HO evolution of the photonic fragmentation functions. Here the nonperturbative contribution at $Q_0=\mu$ is, in principle, nonvanishing and determined via a vector-meson dominance (VMD) ansatz implemented, again, for the DIS$_\gamma$ distributions

$$D_f^\gamma(x,\mu^2)\simeq\frac{4\pi\alpha}{f_\rho^2}D_f^{\rho^0}(x,\mu^2)\ , \tag{4.6}$$

with $f_\rho^2/4\pi\simeq 2.2$, just as in the corresponding spacelike situation [6]. Furthermore, it is expected [5,6] that in the DIS$_\gamma$ factorization scheme this nonperturbative input at $Q_0=\mu$ is similar in the leading and higher perturbative order utilized in the Q^2 evolution of $D_f^\gamma(x,Q^2>\mu^2)$. The magnitude of $D_f^{\rho^0}(x,\mu^2)$ in (4.6) may be inferred from [22] where one notes the small amount of ρ^0 production in e^+e^- annihilation as compared to the much higher rate for π^0 production even at $\sqrt{s}=\sqrt{Q^2}=29$ GeV. Furthermore, since the threshold Q_v for vector-meson production in e^+e^- annihilation via $\gamma^*\to v\pi$, with $v=\rho,\omega,\phi$, satisfies

$$Q_v^2\simeq(m_v+m_\pi)^2\simeq 1\ {\rm GeV}^2\gg\mu^2\ , \tag{4.7}$$

one concludes that

$$D_f^\gamma(x,Q_0^2=\mu^2)=0 \tag{4.8}$$

may be considered as a realistic approximation for the DIS$_\gamma$ distributions which underestimates the true nonperturbative hadronic input rather slightly. To obtain a plausible estimate for the possible upper bound on $D_f^\gamma(x,Q^2)$ we add to the "pointlike" solution, fixed via Eq. (4.8), a VMD inspired hadronic component, utilizing $D_f^{\rho^0}=D_f^{\pi^0}$ as proposed by Field and Feynman [23], with $D_{f,\rm had}^\gamma(x,Q^2)$ obtained from the homogeneous evolution equations [5] using

$$D_{f,\rm had}^\gamma(x,Q^2)=\frac{4\pi\alpha}{f_\rho^2}D_f^{\rho^0}(x,Q^2)\ , \tag{4.9}$$

for the DIS$_\gamma$ distributions superimposed on the pointlike solution. For our calculations we take [24]

$$\begin{aligned}
xD_q^{\rho^0}(x)&=\alpha_v[0.073\sqrt{x}\,(1.703-x)\\
&\qquad+0.188x^{-0.3}(1-x)^2]\ ,\\
xD_{s,\bar s}^{\rho^0}(x)&=\alpha_v[0.188x^{-0.3}(1-x)^2]\ ,\\
xD_g^{\rho^0}(x)&=\alpha_v[0.225x^{-0.3}(1-x)^{1.5}]
\end{aligned} \tag{4.10}$$

at $Q^2\simeq 4$ GeV^2 and where $q=(u,\bar u,d,\bar d)$, $\alpha_v=0.5$. We expect, again in the spirit of the DIS$_\gamma$ scheme, that Eq. (4.9) as combined with (4.10) approximately holds in *both* perturbative orders for the Q^2 evolution of the DIS$_\gamma$ distributions here considered.

It should be emphasized that present experiments do *not* constrain [11] the hadronic distributions in (4.10) below $x\simeq 0.1$ and leave the gluonic fragmentation function $D_g^{\rho^0}=D_g^{\pi^0}$ almost unconstrained. We have therefore chosen, in accordance with the momentum sum rule, a slightly steeper x dependence for the sea and gluon distributions in the small-x region in (4.10) than the flat (*ad hoc*) ansatz of Ref. [24]. This somewhat tames the influence of the small-x singularities in the HO Wilson coefficients [especially $C_g^{(T)}$ in (2.1)] and in the splitting functions on the Q^2 evolutions, similar to the well-known situation for the spacelike parton distributions. Therefore the ansatz (4.10) for the whole x range $0\le x\le 1$ should not be taken too literally and represents at most some "educated guess" which is consistent with all present measurements sensitive to the medium-x region [11,24]. A more detailed quantitative study of these hadronic inputs for D_f^γ requires, of course, measurements of *inclusive* prompt photon production which are not yet available. Presently available data for isolated photon production [1,25,26] can only provide us with some indirect information on the fully inclusive photonic timelike fragmentation functions $D_f^\gamma(x,Q^2)$ whose further investigation affords [11,19] a complete quantitative study of present e^+e^- and $p\bar p$ collider data for isolated, as well as additional data on nonisolated, photon production.

Our DIS$_\gamma$ predictions for D_u^γ and D_g^γ at $Q^2=10^2$ and 10^4 GeV^2 for the situation of unseparated photons ($Q_0^2=\mu^2$), transformed to the $\overline{\rm MS}$ scheme according to Eq. (4.3), are presented in Figs. 5 and 6. Shown are the purely perturbative pointlike (PL) LO and HO results, as obtained from the boundary condition (4.8) in the DIS$_\gamma$ scheme, which, as discussed above, do represent realistic expectations for D_f^γ. We thus do not agree with the estimates of Ref. [11] where large nonperturbative hadronic contributions have been added, based on a huge $D_g^{\pi^0}(x,Q^2)$ which strongly violates the energy-momentum sum rule. A more realistic estimate for a (large) hadronic component is obtained by adding [27] the hadronic input (4.9) to the perturbative pointlike results which is shown by the dashed-dotted and dotted curves for LO and HO, respectively, in Figs. 5 and 6. It should be noted that our purely perturbative pointlike HO predictions for D_u^γ in Fig. 5 are comparable and even larger than the HO results of Ref. [11] (cf. Figs. 10 and 11, dotted and dashed curves) despite the unrealistically large hadronic contribution considered there. Our predictions for D_g^γ in Fig. 6 are, on the other hand, obviously smaller than the corresponding ones of Ref. [11] (cf. Figs. 13 and 14, dotted and dashed curves).

Our LO results could also be compared with the Owens parametrizations [28] currently used for D_q^γ and D_g^γ in the range $x\ge 0.1$, shown by the crosses in Figs. 5 and 6. These correspond to the simple (parameter-free) asymptotic part of the LO pointlike solution where possible hadronic contributions as well as the boundary terms [3,5]

$$[\alpha_s(Q^2)/\alpha_s(Q_0^2)]^{1-2P^{(0)}/\beta_0}$$

are neglected although their purpose is essential to obtain a nonsingular behavior as $x\to 0$. It is therefore not surprising to obtain a difference with respect to our LO results, at least for moderate values of Q^2.

It should finally be noted that the reason for our choice

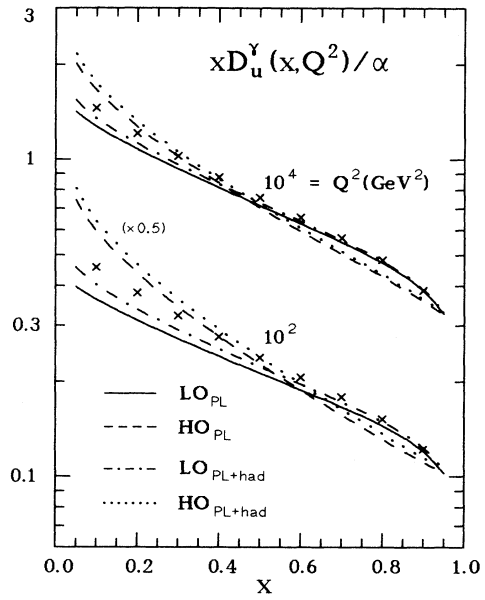

FIG. 5. LO and HO DIS_γ predictions for the photonic fragmentation function $D_u^\gamma(x\equiv z,Q^2)$, corresponding to the pointlike (PL) input at $Q^2=\mu^2$ in (4.8); the additional hadronic (had) contributions have been calculated [27] using the input (4.9)–(4.10). The contributions from the onset of heavy quark thresholds have been included as discussed in the text. The DIS_γ results have been transformed into the $\overline{MS}$ scheme according to (4.3). These predictions are relevant for inclusive direct photon production. The crosses refer to the asymptotic LO solution as parametrized by Owens [28], using $\Lambda=200$ MeV. The results for $Q^2=10^2$ GeV^2 have been multiplied by a factor 0.5.

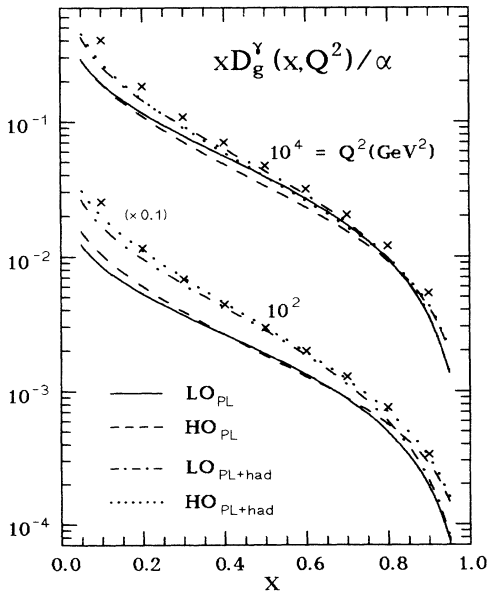

FIG. 6. As in Fig. 5 but for the photonic gluon fragmentation function. The results for $Q^2=10^2$ GeV^2 have been multiplied by a factor 0.1.

of scales in Figs. 4–6 is that $Q=10$ GeV is representative for the theoretically ill understood small-p_T region ($p_T^\gamma \lesssim 20$ GeV) of prompt photon production at collider energies [1,25] while the upper scale $Q=100$ GeV corresponds to the electroweak scale relevant for intermediate-mass Higgs boson searches (via its decay into two photons) at future hadron colliders [29] where an accurate knowledge of the standard QCD background of double-photon production will be of vital importance.

V. SUMMARY AND DISCUSSION

Photon production via deep-inelastic quark and gluon fragmentation into photons is studied beyond the leading order within the framework of a physically motivated factorization scheme (DIS_γ) providing maximal perturbative stability for the Q^2 evolution to be started from an appropriate scale Q_0 which depends on the experimental conditions considered for the observation of the outgoing photon. The perturbative stability is achieved through the elimination of unphysical negative singularities in the HO splitting functions appearing in the artificial, merely mathematical, $\overline{MS}$ factorization scheme. We demonstrate explicitly the elimination of the most conspicuous $\overline{MS}$ singularities not only in the timelike but also in the spacelike region, relevant for the photon structure functions, where these disturbing singularities are somewhat milder.

The analysis of the above-mentioned singularity elimination is most transparent in n-moment space and we provide the required n moments of the HO timelike splitting functions which up to now were only available [13] in fractional momentum x space. Furthermore, a (Mellin) inversion to Bjorken-x (or -z) space is also most convenient for the numerical treatment of the Q^2-evolution equations whose solution in n space can be stated analytically in terms of appropriate boundary conditions at a suitably chosen input scale Q_0. The nonperturbative, VMD-like, hadronic input contribution at Q_0 was argued to be rather negligible under all experimental conditions considered for the observation of the outgoing photon. Under these quite definite vanishing input circumstances at Q_0^2 as prescribed for the isolated [Eq. (4.1)] or nonisolated [Eq. (4.8)] outgoing photon, it turns out that the corresponding, so called "pointlike," predicted distributions are perturbatively stable within the framework of the DIS_γ factorization scheme approach. For the situation of nonisolated photons we also considered the uncertainties involved in the nonperturbative hadronic input [30] by simply adding to the above-mentioned pointlike predictions a further quite extreme hadronic component specified by a VMD ansatz, Eq. (4.9), with $D_f^{\rho^0}=D_f^{\pi^0}$ yielding a possibly exaggerated prediction for the fully inclusive nonisolated photon production rates entailed in D_f^γ. A definitive resolution of the uncertainties related to the appropriate nonperturbative hadronic input involved in the nonisolated photon situation will only be possible by measuring $f_1^{(T)}$ and other related, fully inclusive, quantities at e^+e^- and other (hadronic) high-energy colliders.

It is interesting to note that at $Q^2\simeq 10^4$ GeV^2 the Q_0-

input uncertainties, especially when Q_0 corresponds to a photon-parton isolation cut scale such as $(p_T^{\gamma f})_{\min} \simeq 1$ GeV, are almost washed out due to the long Q^2-evolution distance. This enables a quite reliable estimate of the standard QCD double-photon background encountered in intermediate mass, $m_H \simeq 80-150$ GeV, Higgs boson searches via $H^0 \to \gamma\gamma$ at future [CERN Large Hadron Collider (LHC), Superconducting Super Collider (SSC)] hadron colliders [29]. Here one could also consider more realistic isolation cuts such as a *fixed* $Q_0^2 = O(\delta_{\gamma f}^2 Q^2)$ with $\delta_{\gamma f}$ representing the angular separation between the emitting parton f and the photon. It is mandatory, however, to choose here a z-independent Q_0 and absorb the remaining z dependence, implied by the angular isolation cut kinematics [11,18,19,31], into the HO direct photon production cross section or, alternatively, into the scale Q^2 of the fragmentation functions.

ACKNOWLEDGMENTS

This work has been supported in part by the "Bundesministerium für Forschung und Technologie," Bonn.

APPENDIX A

1. Splitting functions in Bjorken-x space

The HO splitting function $P^{(1)}$ and $k^{(1)}$ in Eqs. (2.9) and (2.10) and the related HO Wilson coefficients in (2.4) and (2.5) depend on the chosen factorization scheme. In our present discussion we adopt the expressions in the $\overline{\text{MS}}$ factorization scheme in Refs. [7–9,11–13]. It should be noted that these expressions differ, for the timelike situation, from the ones in Ref. [14] due to a different unphysical choice of the factorization scheme which does not respect energy-momentum conservation for the quark and gluon fragments [14]. We shall thus only consider the HO timelike expressions in Refs. [8,9,11–13]. The purely hadronic splitting functions in Eqs. (2.9), (2.10), and (2.13) are related, for the flavor singlet case, to the ones in Ref. [13] via

$$\begin{aligned} &P_{gq}^{(i,S)} = P_{FG}^{(i,S)} \ , \quad P_{qg}^{(i,S)} = P_{GF}^{(i,S)} \ , \\ &P_{gq}^{(i,T)} = 2f P_{FG}^{(i,T)} \ , \quad P_{qg}^{(i,T)} = (2N_F)^{-1} P_{GF}^{(i,T)} \ , \end{aligned} \tag{A1}$$

where $N_F \equiv f$ and $i = 0, 1$; the diagonal singlet elements in (2.13) are as in Ref. [13] with [32] $F \to q$ and $G \to g$. The relevant nonsinglet splitting function is, in HO, given by $P_+^{(1)}$ in Eqs. (4.8) and (4.50)–(4.55) of Ref. [12].

The photonic spacelike ($\gamma \to q, \gamma \to g$) and timelike ($q \to \gamma, g \to \gamma$) splitting functions $k^{(S)}$ and $k^{(T)}$ in (2.9) and (2.10), respectively, are obtained from the purely hadronic $P_{ij}^{(S,T)}$ by an obvious replacement of the color factors [3] and an elimination of the $\delta(1-x)$ terms in $P_{gg}^{(1)}$ which do not contribute [5,10] to the off-diagonal γg elements $k_g^{(1)}$. This finally yields, in LO,

$$\begin{aligned} &f(e_q^2 - \langle e^2 \rangle)^{-1} k_{NS,q}^{(0,S)} = \langle e^2 \rangle^{-1} k_q^{(0,S)} = 3T_R^{-1} P_{qg}^{(0,S)} \ , \\ &f(e_q^2 - \langle e^2 \rangle)^{-1} k_{NS,q}^{(0,T)} = \langle e^2 \rangle^{-1} k_q^{(0,T)} = C_F^{-1} P_{gq}^{(0,T)} \ , \\ &k_g^{(0,S)} = k_g^{(0,T)} = 0 \ , \end{aligned} \tag{A2}$$

and, for the HO photonic splitting functions in the $\overline{MS}$ factorization scheme,

$$\begin{aligned} f(e_q^2 - \langle e^2 \rangle)^{-1} k_{NS,q}^{(1,S)} &= \langle e^2 \rangle^{-1} k_q^{(1,S)} \\ &= 3FC_f \{ 4 - 9x - (1-4x)\ln x - (1-2x)\ln^2 x + 4\ln(1-x) \\ &\quad + [4\ln x + 2\ln^2 x - 4\ln x \ln(1-x) - 4\ln(1-x) \\ &\quad + 2\ln^2(1-x) - \tfrac{2}{3}\pi^2 + 10][x^2 + (1-x)^2] \} \ , \\ f(e_q^2 - \langle e^2 \rangle)^{-1} k_{NS,q}^{(1,T)} &= \langle e^2 \rangle^{-1} k_q^{(1,T)} \\ &= 2fC_F \{ -\tfrac{1}{2} + \tfrac{9}{2}x - (8 - \tfrac{1}{2}x)\ln x + 2x \ln(1-x) + (1 - \tfrac{1}{2}x)\ln^2 x \\ &\quad + [\ln^2(1-x) + 4\ln x \ln(1-x) - 8S_1(x) - \tfrac{4}{3}\pi^2][1 + (1-x)^2]x^{-1} \} \ , \\ k_g^{(1,S)} &= 3f\langle e^2 \rangle C_F \left[-16 + 8x + \frac{20}{3}x^2 + \frac{4}{3x} - (6 + 10x)\ln x - 2(1+x)\ln^2 x \right] \ , \\ k_g^{(1,T)} &= f\langle e^2 \rangle T_R \left[-4 + 12x - \frac{164}{9}x^2 + \frac{92}{9x} + \left[10 + 14x + \frac{16}{3}x^2 + \frac{16}{3x} \right] \ln x + 2(1+x)\ln^2 x \right] \ , \end{aligned} \tag{A3}$$

where

$$S_1(x) \equiv -Li_2(1-x) = \int_0^{1-x} \frac{dz}{z} \ln(1-z) \ ,$$

$C_F = \frac{4}{3}$, $T_R = \frac{1}{2}$, and $\langle e^2 \rangle \equiv f^{-1} \sum_f e_q^2$, with f being the number of active light quark flavors.

The evaluation of the convolutions in (2.14), required for the transformation to the DIS_γ factorization scheme, can be performed analytically using standard Mellin integrals [5]. Since our numerical integrations of the evolution equations is performed for the analytic solutions in the Mellin n-moment space [5,16], we refrain from

presenting here the corresponding explicit x-space expressions for the timelike quantities in (2.14).

2. Moments of splitting functions and coefficient functions

The moments of the LO splitting functions are well known: $P_{ij}^{(0,S)}(n)=-\gamma_{ij}^{(0)n}/4$ for the spacelike case with $\gamma_{ij}^{(0)n}$ given by Eqs. (B.14)–(B.17) of Ref. [14]; the diagonal quantities are universal, i.e., $P_{qq}^{(0,T)}(n)=P_{qq}^{(0,S)}(n)$ and $P_{gg}^{(0,T)}(n)=P_{gg}^{(0,S)}(n)$, whereas the timelike off-diagonal elements, given by (A1), are $P_{gq}^{(0,T)}(n)=2fP_{gq}^{(0,S)}(n)$ and $P_{qg}^{(0,T)}(n)=(2f)^{-1}P_{qg}^{(0,S)}(n)$. This also fixes the moments of the photonic LO splitting functions in Eq. (A2).

The moments of the spacelike HO splitting functions are known as well:

$$P_{\mathrm{NS}+}^{(1,S)}(n)=-\gamma_{\mathrm{NS}}^{(1)n}(\eta=+1)/8\ ,\qquad P_{ij}^{(1,S)}(n)=-\gamma_{ij}^{(1)n}/8 \tag{A4}$$

with $\gamma_{\mathrm{NS}}^{(1)n}$ $(\eta=+1)$ and $\gamma_{ij}^{(1)n}$ given by Eqs. (B.18) and (B.19)–(B.22) of Ref. [14], respectively. The moments $k_q^{(1,S)}(n)$ and $k_g^{(1,S)}(n)$ of the photonic HO splitting functions in (A3) can be found in Ref. [5], Eqs. (2.9) and (2.10), respectively. Similarly, the moments of the spacelike Wilson coefficients in Eqs. (2.4) and (2.5) are given by $C_{q,2}^{(S)}(n)=B_q^n/2$ and $C_{g,2}^{(S)}(n)=B_G^n/4f$ with B_q^n and B_G^n given by Eq. (2.20) of Ref. [5], and

$$C_{q,1}^{(S)}(n)=C_{q,2}^{(S)}(n)-C_F\frac{2}{n+1}\ ,\qquad C_{g,1}^{(S)}(n)=C_{g,2}^{(S)}(n)-T_R\left[\frac{4}{n+1}-\frac{4}{n+2}\right] \tag{A5}$$

according to Eqs. (2.4) and (2.5). The moments of $C_{\gamma,r}^{(S)}$ are then fixed via (2.6).

The moments of the relevant timelike HO splitting functions of Ref. [13] have not been calculated so far. A straightforward but tedious calculation of the Mellin moments of $P_{ij}^{(1,T)}(x)$ in (A1) yields

$$P_{\mathrm{NS}+}^{(1,T)}(n)=P_{\mathrm{NS}+}^{(1,S)}(n)+C_F^2\left[-4S_1(n)+3+\frac{2}{n(n+1)}\right]\left[2S_2(n)-\frac{\pi^2}{3}-\frac{2n+1}{n^2(n+1)^2}\right], \tag{A6}$$

$$\begin{aligned}P_{qq}^{(1,T)}(n)=&P_{qq}^{(1,S)}(n)+C_F^2\left[-4S_1(n)+3+\frac{2}{n(n+1)}\right]\left[2S_2(n)-\frac{\pi^2}{3}-\frac{2n+1}{n^2(n+1)^2}\right]\\&+C_FT_Rf\left[-\frac{80}{9}\frac{1}{n-1}+\frac{8}{n^3}+\frac{12}{n^2}-\frac{12}{n}+\frac{8}{(n+1)^3}+\frac{28}{(n+1)^2}-\frac{4}{n+1}+\frac{32}{3}\frac{1}{(n+2)^2}+\frac{224}{9}\frac{1}{n+2}\right],\end{aligned} \tag{A7}$$

$$\begin{aligned}2fP_{qg}^{(1,T)}(n)=&(T_Rf)^2\frac{8}{3}\left[S_1(n+1)\frac{n^2+n+2}{n(n+1)(n+2)}+\frac{1}{n^2}-\frac{5}{3}\frac{1}{n}-\frac{1}{n(n+1)}-\frac{2}{(n+1)^2}+\frac{4}{3}\frac{1}{n+1}\right.\\&\left.+\frac{4}{(n+2)^2}-\frac{4}{3}\frac{1}{n+2}\right]\\&+C_FT_Rf\left[[-2S_1^2(n+1)+2S_1(n+1)+10S_2(n+1)]\frac{n^2+n+2}{n(n+1)(n+2)}\right.\\&+4S_1(n+1)\left[-\frac{1}{n^2}+\frac{1}{n}+\frac{1}{n(n+1)}+\frac{2}{(n+1)^2}-\frac{4}{(n+2)^2}\right]\\&-\frac{2}{n^3}+\frac{5}{n^2}-\frac{12}{n}+\frac{4}{n^2(n+1)}-\frac{12}{n(n+1)^2}-\frac{6}{n(n+1)}\\&\left.+\frac{4}{(n+1)^3}-\frac{4}{(n+1)^2}+\frac{23}{n+1}-\frac{20}{n+2}\right]\\&+C_GT_Rf\left[\left[2S_1^2(n+1)-\frac{10}{3}S_1(n+1)-6S_2(n+1)+2G^{(1)}(n+1)-\pi^2\right]\frac{n^2+n+2}{n(n+1)(n+2)}\right.\\&-4S_1(n+1)\left[-\frac{2}{n^2}+\frac{1}{n}+\frac{1}{n(n+1)}+\frac{4}{(n+1)^2}-\frac{6}{(n+2)^2}\right]-\frac{40}{9}\frac{1}{n-1}+\frac{4}{n^3}+\frac{8}{3}\frac{1}{n^2}\\&+\frac{26}{9}\frac{1}{n}-\frac{8}{n^2(n+1)^2}+\frac{22}{3}\frac{1}{n(n+1)}+\frac{16}{(n+1)^3}+\frac{68}{3}\frac{1}{(n+1)^2}-\frac{190}{9}\frac{1}{n+1}\\&\left.+\frac{8}{(n+1)^2(n+2)}-\frac{4}{(n+2)^2}+\frac{356}{9}\frac{1}{n+2}\right],\end{aligned} \tag{A8}$$

$$
\begin{aligned}
(2f)^{-1}P_{gq}^{(1,T)}(n)=C_F^2\Bigg[&\left[S_1^2(n)-3S_2(n)-\frac{2\pi^2}{3}\right]\frac{n^2+n+2}{(n-1)n(n+1)}\\
&+2S_1(n)\left[\frac{4}{(n-1)^2}-\frac{2}{(n-1)n}-\frac{4}{n^2}+\frac{3}{(n+1)^2}-\frac{1}{n+1}\right]-\frac{8}{(n-1)^2n}+\frac{8}{(n-1)n^2}\\
&+\frac{2}{n^3}+\frac{8}{n^2}-\frac{1}{2n}+\frac{1}{(n+1)^3}-\frac{5}{2}\frac{1}{(n+1)^2}+\frac{9}{2}\frac{1}{n+1}\Bigg]\\
+C_FC_G\Bigg[&\left[-S_1^2(n)+5S_2(n)-G^{(1)}(n)+\frac{\pi^2}{6}\right]\frac{n^2+n+2}{(n-1)n(n+1)}\\
&+2S_1(n)\left[-\frac{2}{(n-1)^2}+\frac{2}{(n-1)n}+\frac{2}{n^2}-\frac{2}{(n+1)^2}+\frac{1}{n+1}\right]-\frac{8}{(n-1)^3}\\
&+\frac{6}{(n-1)^2}+\frac{17}{9}\frac{1}{n-1}+\frac{4}{(n-1)^2n}-\frac{12}{(n-1)n^2}-\frac{8}{n^2}+\frac{5}{n}-\frac{2}{n^2(n+1)}-\frac{2}{(n+1)^3}\\
&-\frac{7}{(n+1)^2}-\frac{1}{n+1}-\frac{8}{3}\frac{1}{(n+2)^2}-\frac{44}{9}\frac{1}{n+2}\Bigg],
\end{aligned}
\tag{A9}
$$

$$
\begin{aligned}
P_{gg}^{(1,T)}(n)=P_{gg}^{(1,S)}(n)+C_FT_Rf\Bigg[&-\frac{16}{3}\frac{1}{(n-1)^2}+\frac{80}{9}\frac{1}{n-1}+\frac{8}{n^3}-\frac{16}{n^2}+\frac{12}{n}+\frac{8}{(n+1)^3}-\frac{24}{(n+1)^2}\\
&+\frac{4}{n+1}-\frac{16}{3}\frac{1}{(n+1)^2}-\frac{224}{9}\frac{1}{n+2}\Bigg]\\
+C_GT_Rf\left[-\frac{8}{3}\right]&\left[S_2(n)-\frac{1}{(n-1)^2}+\frac{1}{n^2}-\frac{1}{(n+1)^2}+\frac{1}{(n+2)^2}-\frac{\pi^2}{6}\right]\\
+C_G^2\Bigg[&-8S_1(n)S_2(n)+8S_1(n)\left[\frac{1}{(n-1)^2}-\frac{1}{n^2}+\frac{1}{(n+1)^2}-\frac{1}{(n+2)^2}+\frac{\pi^2}{6}\right]\\
&+\left[8S_2(n)-\frac{4\pi^2}{3}\right]\left[\frac{1}{n-1}-\frac{1}{n}+\frac{1}{n+1}-\frac{1}{n+2}+\frac{11}{12}\right]-\frac{8}{(n-1)^3}+\frac{22}{3}\frac{1}{(n-1)^2}-\frac{8}{(n-1)^2n}\\
&-\frac{8}{(n-1)n^2}-\frac{8}{n^3}-\frac{14}{3}\frac{1}{n^2}-\frac{8}{(n+1)^3}+\frac{14}{3}\frac{1}{(n+1)^2}-\frac{8}{(n+1)^2(n+2)}-\frac{8}{(n+1)(n+2)^2}\\
&-\frac{8}{(n+2)^3}-\frac{22}{3}\frac{1}{(n+2)^2}\Bigg],
\end{aligned}
\tag{A10}
$$

with the $P_{ij}^{(1,S)}(n)$ given by Eq. (A4), $C_F=\frac{4}{3}, T_R=\frac{1}{2}$, $C_G=3$, and

$$
S_k(n)\equiv\sum_{j=1}^{n}\frac{1}{j^k}\ ,\quad G^{(1)}(n)\equiv\frac{d}{dn}\left[\psi\left[\frac{n+1}{2}\right]-\psi\left[\frac{n}{2}\right]\right],
\tag{A11}
$$

where $\psi(z)=d\ln\Gamma(z)/dz$, and the analytic continuation in n, required for the Mellin inversion to the Bjorken-x space, are well known [5]. The moments of the photonic splitting functions $k^{(1,T)}(x)$ in the $\overline{\text{MS}}$ scheme as presented in (A3) are then

$$f(e_q^2-\langle e^2\rangle)^{-1}k_{NS,q}^{(1,T)}(n)=\langle e^2\rangle^{-1}k_q^{(1,T)}(n)$$
$$=2fC_F\left[\left[S_1^2(n)-3S_2(n)-\frac{2\pi^2}{3}\right]\frac{n^2+n+2}{(n-1)n(n+1)}\right.$$
$$+2S_1(n)\left[\frac{4}{(n-1)^2}-\frac{2}{(n-1)n}-\frac{4}{n^2}+\frac{3}{(n+1)^2}-\frac{1}{n+1}\right]-\frac{8}{(n-1)^2n}$$
$$\left.+\frac{8}{(n-1)n^2}+\frac{2}{n^3}+\frac{8}{n^2}-\frac{1}{2n}+\frac{1}{(n+1)^3}-\frac{5}{2}\frac{1}{(n+1)^2}+\frac{9}{2}\frac{1}{n+1}\right], \tag{A12}$$

$$k_g^{(1,T)}(n)=f\langle e^2\rangle T_R\left[-\frac{16}{3}\frac{1}{(n-1)^2}+\frac{92}{9}\frac{1}{n-1}+\frac{4}{n^3}-\frac{10}{n^2}-\frac{4}{n}+\frac{4}{(n+1)^3}-\frac{14}{(n+1)^2}\right.$$
$$\left.+\frac{12}{n+1}-\frac{16}{3}\frac{1}{(n+2)^2}-\frac{164}{9}\frac{1}{n+2}\right]. \tag{A13}$$

Finally, the moments of the timelike Wilson coefficients in Eqs. (2.4) and (2.5) are given by

$$C_{q,2}^{(T)}(n)=C_F\left[5S_2(n)+S_1^2(n)+S_1(n)\left[\frac{3}{2}-\frac{1}{n(n+1)}\right]-\frac{2}{n^2}-\frac{2}{n}+\frac{3}{(n+1)^2}-\frac{3}{2}\frac{1}{n+1}-\frac{9}{2}\right],$$
$$C_{q,1}^{(T)}(n)=C_{q,2}^{(T)}(n)+C_F(2/n),$$
$$C_{g,2}^{(T)}(n)=C_F\left[-S_1(n)\frac{n^2+n+2}{(n-1)n(n+1)}-\frac{4}{(n-1)^2}-\frac{4}{(n-1)n}+\frac{4}{n^2}-\frac{3}{(n+1)^2}\right], \tag{A14}$$
$$C_{g,1}^{(T)}(n)=C_{g,2}^{(T)}(n)+C_F\frac{4}{(n-1)n},$$

which fixes also the moments of $C_{\gamma,r}^{(T)}$ via the relation (2.6).

Utilizing these moments of timelike splitting functions, one can use the Q^2-evolution formalism and the analytic solutions for the spacelike situation of Ref. [5] without modification by noting the correspondence between $\hat{P}^{(S)}$ and $\hat{P}^{(T)}$ presented in (2.13), and by the replacements $k^{(i,S)}\to k^{(i,T)}$, $q^\gamma(n,Q^2)\to D_q^\gamma(n,Q^2)$ and $g^\gamma(n,Q^2)\to D_g^\gamma(n,Q^2)$.

[1] Collider Detector at Fermilab Collaboration, F. Abe *et al.*, Phys. Rev. Lett. **68**, 2734 (1992).

[2] E. Pilon, in '91 *High Energy Hadronic Interactions,* Proceedings of the 26th Rencontre de Moriond, Les Arcs, France, 1991, edited by J. Tran Thanh Van (Editions

[3] M. Glück and E. Reya, Phys. Rev. D **28**, 2749 (1983).

[4] M. Glück, K. Grassie, and E. Reya, Phys. Rev. D **30**, 1447 (1984).

[5] M. Glück, E. Reya, and A. Vogt, Phys. Rev. D **45**, 3986 (1992).

[6] M. Glück, E. Reya, and A. Vogt, Phys. Rev. D **46**, 1973 (1992).

[7] G. Altarelli, R. K. Ellis, and G. Martinelli, Nucl. Phys. **B157**, 461 (1979).

[8] G. Altarelli, R. K. Ellis, G. Martinelli, and S.-Y. Pi, Nucl. Phys. **B160**, 301 (1979).

[9] W. Furmanski and R. Petronzio, Z. Phys. C **11**, 293 (1982). There is a printing error in Appendix 2 in the timelike fermionic Wilson coefficient, which we have corrected in our Eq. (2.4).

[10] M. Fontannaz and E. Pilon, Phys. Rev. D **45**, 382 (1992).

[11] P. Aurenche, P. Chiappetta, M. Fontannaz, J. Ph. Guillet, and E. Pilon, Report No. LPTHE-Orsay 92/30, Nucl. Phys. B (to be published).

[12] G. Curci, W. Furmanski, and R. Petronzio, Nucl. Phys. **B175**, 27 (1980).

[13] W. Furmanski and R. Petronzio, Phys. Lett. **97B**, 437 (1980).

[14] E. G. Floratos, C. Kounnas, and R. Lacaze, Nucl. Phys. **B192**, 417 (1981).

[15] M. Diemoz, F. Ferroni, E. Longo, and G. Martinelli, Z. Phys. C **39**, 21 (1988).

[16] M. Glück, E. Reya, and A. Vogt, Z. Phys. C **48**, 471 (1990).

[17] M. Glück, E. Reya, and A. Vogt, Phys. Lett. B **285**, 285 (1992).

[18] P. Aurenche, R. Baier, M. Fontannaz, and D. Schiff, Nucl. Phys. **B297**, 661 (1988); P. Aurenche, R. Baier, and M. Fontannaz, Phys. Rev. D **42**, 1440 (1990).

[19] E. L. Berger and J. Qiu, Phys. Rev. D **44**, 2002 (1991).

[20] Alternatively, one could of course also work in the DIS_γ scheme, but this requires the more complicated transformations of the $\overline{\mathrm{MS}}$ photon-parton subprocess cross sections to the DIS_γ scheme [5].

[21] P. Aurenche, P. Chiappetta, M. Fontannaz, J. Ph. Guillet, and E. Pilon, Z. Phys. C **56**, 589 (1992).

[22] Particle Data Group, K. Hikasa *et al.*, Phys. Rev. D **45**, S1 (1992); W. Hofmann, Annu. Rev. Nucl. Part. Sci. **38**, 279 (1988).

[23] R. D. Field and R. P. Feynman, Nucl. Phys. **B136**, 1

(1978).
[24] J. F. Owens, Phys. Rev. D **19**, 3279 (1979).
[25] UA2 Collaboration, J. Alitti *et al.*, Phys. Lett. B **263**, 544 (1991).
[26] ALEPH Collaboration, D. Decamp *et al.*, Phys. Lett. B **264**, 476 (1991).
[27] Contrary to the perturbative (pointlike) part, where the charm contribution is nonvanishing for $Q^2 > m_C^2 = (1.5\ \mathrm{GeV})^2$, the hadronic charm contribution is neglected below the input scale [24] $Q^2 = 4\ \mathrm{GeV}^2$ in Eq. (4.10) which, strictly speaking, is not absolutely correct but numerically insignificant.
[28] J. F. Owens, Rev. Mod. Phys. **59**, 465 (1987).
[29] See, for example, Z. Kunszt, in Perspectives in Higgs Physics (World Scientific, Singapore, to be published).
[30] The formalism developed here, in particular the calculation of the moments of two-loop anomalous dimensions, should prove useful for future HO analyses of purely hadronic fragmentation functions $D_{q,g}^h(z,Q^2)$, obeying conventional homogeneous evolution equations [i.e., $k^{(T)} \equiv 0$ in Eq. (2.9)], which will be important for a fully consistent HO analysis of semi-inclusive particle production [see, for example, F. M. Borzumati, B. A. Kniehl, and G. Kramer, Z. Phys. C **57**, 595 (1993).
[31] H. Baer and J. F. Owens, Phys. Lett. B **205**, 377 (1988); B. Bailey, J. F. Owens, and J. Ohnemus, Phys. Rev. D **46**, 2018 (1992); Z. Kunszt and Z. Trócsányi, Nucl. Phys. **B394**, 139 (1993).
[32] It should be noted that there is a printing error in the $C_F T_R N_F$ term of $\hat{P}_{FF}^{(1,T)}$ in Eq. (12) of Ref. [13]: The term $(10-18x-16x^2/3)\ln x$ should correctly read $(-10-18x-16x^2/3)\ln x$.